Gamow-Teller strengths of some sd-shell nuclei in the shell model framework

S. M. Obaid and H. M. Tawfeek
Department of Physics, College of Education for Pure Science (Ibn-Alhaitham), University of Baghdad, Baghdad, Iraq.

Received 14 November 2019; accepted 20 February 2020

The nuclear Gamow-Teller (GT) transition strength distributions *B(GT)* have been studied for some sd-shell nuclei in the (^{3}He, t) charge-exchange reactions. The shell model calculations were performed by employing the USDA and USDB effective interactions in the sd-model space. We performed the calculations for ^{24}Mg→^{24}Al, ^{24}Mg →^{24}Na, ^{25}Mg →^{25}Al, ^{26}Mg→^{26}Na, and ^{26}Mg→^{26}Al. The results of B(GT) calculations were compared to the experimental Gamow-Teller strength distributions and with previous study and they were found in reasonable agreement. The calculated distribution of summed GT transition strengths are in acceptable global agreement compared to the experimental data.

Keywords: Gamow-Teller transitions; charge-exchange reactions; isospin symmetry.

PACS: 26.50.+x; 25.40.Kv; 23.20.Nx DOI: https://doi.org/10.31349/RevMexFis.66.330

1. Introduction

The Gamow-Teller (GT) transition is without doubt one of spin-isosopin ($\sigma\tau$) type's most prominent nuclear weak transitions. They are not only involved in nuclear physics, they also play an important part in supernova explosions and nuclear synthesis. The GT reaction of core elements in the medium-mass region (MMR) is important to assess the pre-collapse production of supernova [1–4]. Electron capture reaction and β-decay were significant nuclear processes at the beginning of the supernova core collapse [5-7]. Transitions of GT with $\Delta J^\pi = 1^+$ are mediated by a single $\sigma\tau$ operator and therefore do not have an orbital angular-momentum transfer ($\Delta L = 0$) and spin-isospin flip-type ($\Delta S = 1$ and ΔT=1). Therefore, GT± transitions are of type T_z = ±1, where T_z is the third component of the isospin T which is given by $T = (N - Z)/2$ [8–10].

Saxena *et al.*, conducted two $ab\ initio$ approaches namely: The in-medium similarity renormalization group (IM-SRG) [19] and the coupled-cluster effective interaction (CCEI) to study of the strengths distributions of the transition strength of Gamow-Teller in some selected sd-shell nuclei. They also compared their theoretical results from the two mentioned approaches with the shell model calculations using the phenomenological USDB effective interaction [11]. Zegers *et al.*, studied [12] the ^{24}Mg(^{3}He,t)^{24}Al reaction at $E(^3$He)=420 MeV. An energy resolution of 35 keV was achieved. A recently developed empirical relation for proportionalities between Gamow-Teller and differential cross sections was used to extract Gamow-Teller strengths to discrete levels in ^{24}Al. In the $T = 1/2$ mirror nuclei pair ^{23}Na-^{23}Mg. Fujita *et al.*, studied the contribution of these different conditions, comparing the strengths of analog gamma M1 transitions and GT transitions deduced from high-resolution ^{23}Na(^{3}He,t)^{23}Mg charge-exchange measurements [13].

This study is aimed to calculate the GT strength distributions with higher energies of excitation. This could be very useful for future experimental data. The shell model calculations will be conducted using the shell model code NuShellX@MSU [14] to obtain the GT-strengths for ^{24}Mg→^{24}Al, ^{24}Mg →^{24}Na, ^{25}Mg →^{25}Al, ^{26}Mg→ ^{26}Na, and ^{26}Mg→^{26}Al using USDA and USDB effective interactions in the full sd-model space. The results $B(GT)$ values and their summed $B(GT)$ will be compared with the corresponding experimental data.

2. Theoretical framework

The transitions are formed of two kinds under the selection rules for parity and angular momentum: GT transitions of Fermi (vector) and (axial-vector). Fermi transitions occur in a daughter nucleus only in isospin analog states where spin and parity are preserved (under conservation of isospin), *i.e.*, $|\Delta J = J_i - J_f| = 0$, $\Delta\pi = \pi_i\pi_f = +1$. The GT transition must satisfy the condition $|\Delta J = J_i - J_f| = 0, \pm 1$, $\Delta\pi = \pi_i\pi_f = +1$, (excluding $0^+ \rightarrow 0^+$). A shell model calculations without restriction were performed to describe the strengths distribution of the measured GT for sd-shell nuclei in the sd model space with USDA and USDB effective interactions [15]. The reduced GT transition strength $B(GT)$ for the transition from the initial state with spin J_i, isospin T_i, and $z-$component of isospin T_{zi} to the final state with J_f, T_f, and T_{zf} is given by [16]

$$B^{\pm}(GT) = \frac{1}{2J_i+1} \times \left| \langle J_f T_f T_{zf} \| \frac{1}{\sqrt{2}} \sum_{j=1}^{A} (\sigma_j \tau_j^{\pm}) \| J_i T i T_{zi} \rangle \right|^2 , \quad (1)$$

where $\tau^{\pm 1} = \mp(1/\sqrt{2})(\tau_x + i\tau_y)$ and a rank one tensor transform , and $T_z = (N - Z)/2$. By employing the theorem of Wigner-Eckart in the space of the isospin, we get

$$B(GT) = \frac{1}{2J_i+1}\frac{1}{2}\frac{C^2}{2T_f+1}\left|\langle J_f T_f \| \sum_{i=1}^{A}(\sigma_j\tau_j)\| J_i T_i\rangle\right|^2$$
$$= \frac{1}{2J_i+1}\frac{1}{2}\frac{C^2}{2T_f+1}\left[M_{GT}(\sigma\tau)\right]^2, \qquad (2)$$

where C_{GT} is the isospin Clebsch-Gordan (CG) coefficient $(T_iT_{zi} \pm 1|T_fT_{zf})$ and the $M_{GT}(\sigma\tau)$ is the GT matrix element of isovector spin-type.

From this expression for the "reduced" GT transition strength, we see that $B(GT)$ consists matrix element of squared value of the isovector spin operator $M_{GT}(\sigma\tau)$ and spin and isospin geometrical factors. Therefore, even if initial and final states are common, then the transitions are different $B(GT)$ values in reversed directions. For example, the GT transition from a state having $|JTT_z\rangle$ of $|0T_0T_0\rangle$ to the $|1T_0 - 1T_0 - 1\rangle$ state has three times larger $B(GT)$ than that in the reverse direction.

3. Results and Discussion

3.1. ^{24}Mg $\rightarrow^{24}$Al

Figure 1 displays the calculated and measured strength distributions of $B(GT)$ for the transition ^{24}Mg $\rightarrow^{24}$Al. The $B(GT)$ values from ground state of ^{24}Mg (0^+)-$\rightarrow^{24}$Al(1^+) states without any truncation using USDA and USDB interactions were calculated. The experimental data observed through the ^{24}Mg(^{3}He,t)^{24}Al charge-exchange reaction observed at 420 MeV [17] and ^{24}Mg(p,n)^{24}Al reaction observed at 136 MeV [18]. Our results using USDA and USDB interactions agrees very well with the previous study conducted by [17] using USDA and USDB effective interactions. Also, our work agrees very well with the work of Saxena *et al*. [11]

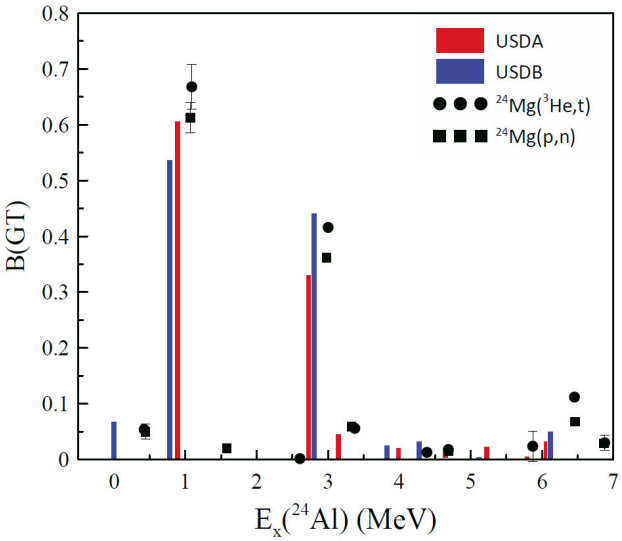

FIGURE 1. Shows the theoretical values $B(GT)$ in comparison to the corresponding experimental data [17, 18] for ^{24}Mg.

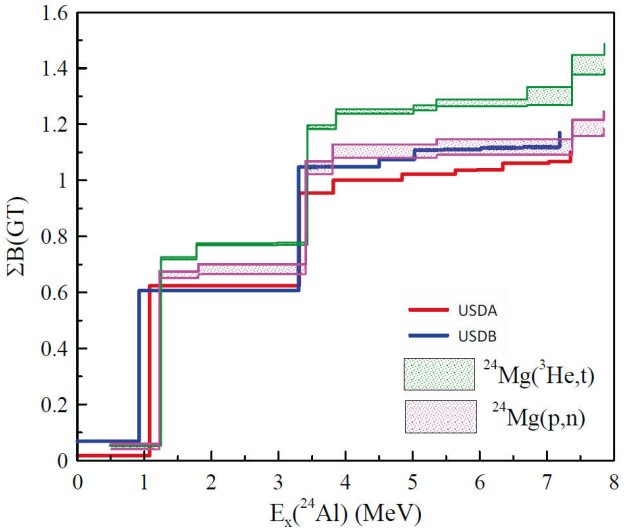

FIGURE 2. Shows the $\sum B(GT)$ distributions compared to experiment [17, 18] for ^{24}Mg.

using different theoretical techniques. There are two dominant peaks at $E_x(^{24}\text{Al})$= 0.889 MeV and $E_x(^{24}\text{Al})$= 2.726 MeV with values 0.606 and 0.331, respectively, for USDA interaction. The two dominant peaks for USDB interaction located at $E_x(^{24}\text{Al})$= 0.783 MeV and $E_x(^{24}\text{Al})$= 2.805 MeV with values 0.537 and 0.441, respectively. Figure 2 represents the running sums of $B(GT)$ versus excitation energy $E_x(^{24}\text{Al})$. The strongest peaks for the ^{24}Mg(^{3}He,t)^{24}Al reactions observed at 1.090 MeV and 3.001 MeV with values 0.668 and 0.416, respectively. The strongest peaks for ^{24}Mg(p,n)^{24}Al reaction are found at 1.07 MeV and 2.98 MeV with values 0.613 and 0.362, respectively. The first and second strongest peaks calculated from USDA and USDB interactions comes from the transitions ^{24}Mg $(0^+) \rightarrow^{24}$Al(1^+_2) and ^{24}Mg $(0^+) \rightarrow^{24}$Al(1^+_3), respectively. The USDA and USDB interactions predicts correctly the ground state at 4^+ which agrees with experimental observation. The accumulated sums of $B(GT)$ given by USDA and USDB interactions are in better agreement with ^{24}Mg(p,n)^{24}Al reaction than ^{24}Mg(^{3}He,t)^{24}Al reaction. The shell model resulting from both interactions is capable of explaining the observed GT transition strength concentrated at the energy of lowest excitation. Overall, the results of the shell model explained successfully the gross characteristics of the experimental $B(GT)$ values as well as the summed $B(GT)$ strengths.

3.2. ^{24}Mg $\rightarrow^{24}$Na

Figure 3 shows the shell model and GT strength experimental data for the ^{24}Mg $\rightarrow^{24}$Na transition. The B(GT) values were determined from ground state of ^{24}Mg $(0^+$ to ^{24}Na $(1^+$ states) without any truncation using USDA and USDB interactions. The are three experimental data available from ^{24}Mg(^{3}He, t)^{24}Na [12], ^{24}Mg(d,^{2}He)^{24}Na [17] and ^{24}Mg(t, ^{3}He)^{24}Na [19] through the charge-exchange reaction the experimental data. The strongest peak

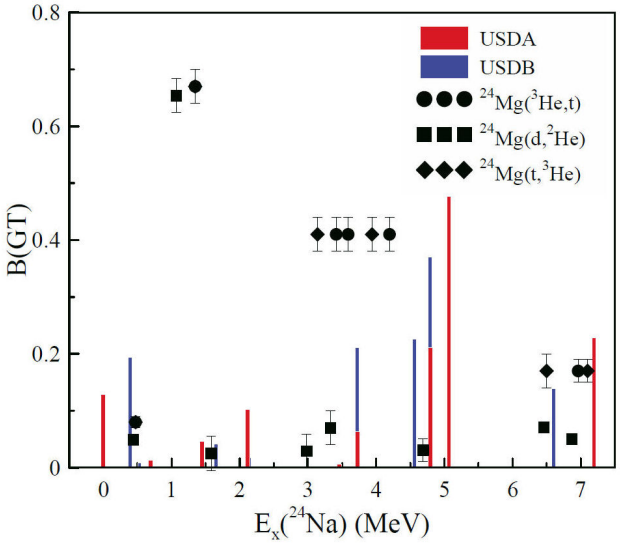

FIGURE 3. Shows the theoretical values of $B(GT)$ compared to the corresponding experimental data [12, 17, 19] for ^{24}Mg. The experimental data taken from.

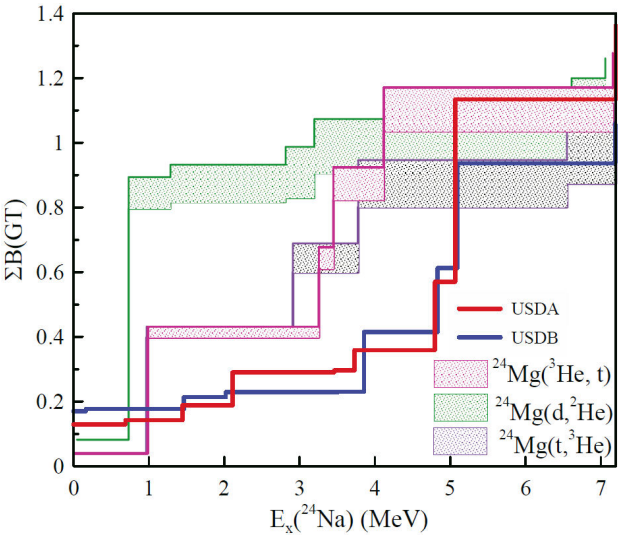

FIGURE 4. Shows the $\sum B(GT)$ distributions compared to experiment [12, 17, 19] for ^{24}Mg.

in the observed experimental data for ^{24}Mg(^{3}He,t)^{24}Na reaction is located at $E_x(^{24}\text{Na})$=1.346 MeV with value 0.67 and the rest distribution of $B(GT)$ lies in energy range $E_x(^{24}\text{Na})$-=3.14-3.94 MeV and $E_x(^{24}\text{Na})$=7.1 MeV. The strongest peak for the reaction ^{24}Mg(t,^{3}He)^{24}Na is found at $E_x(^{24}\text{Na})$=1.07 MeV with value 0.654 and the rest six values below 1 distributed in the range $E_x(^{24}\text{Na})$=0.44-6.87 MeV. The shell model calculations using USDA and USDB are quenched by a factor 0.59 to account for combination of configuration mixing with 2p-2h states as done in Ref. [12]. The strongest beaks found by USDA and USDB interactions are located at 5.067 MeV and 4.952 MeV with $B(GT)$ values 0.564 and 0.37, respectively. These strong peaks predicted by USDA and USDB comes from the transition ^{24}Mg (0^+)-$\rightarrow^{24}$Na(1^+_9). The ground state of ^{24}Na=4^+ is correctly predicted by both USDA and USDB interactions. Figure 4 displays the $B(GT)$ running sums in terms of excitation energy E_x of ^{24}Na . The intensities calculated are similar to those measured for this transition. It is seen that the USDA and USDB interactions predicted the excitation energy agreed with the experimental data, the summed strength $B(GT)$ as shown in Fig. 4 is closer to the experiment than the USDB interaction with the summed $B(GT)$. The USDA and USDB accumulated sum of B(GT) strength calculations is in line with the experiment on higher excitation energy $E_x(^{24}\text{Na}) \geq$ 5 MeV, but not on low excitation energy $E_x(^{24}\text{Na}) < 5$ MeV, overall the summed $B(GT)$ strength predicted by USDA interaction better than USDB matched with observed ones.

3.3. ^{25}Mg $\rightarrow^{25}$Al

Figure 5 displays the calculated and the measured $B(GT)$ strength distributions for the transition $^{25}\text{Mg}(5/2^+) \rightarrow {}^{25}\text{Al}(3/2^+, 5/2^+, 7/2^+)$ without any truncation. The measured data observed through the reaction of charge-exchange ^{25}Mg (^{3}He,t) ^{25}Al [22, 23]. The dominant B(GT) in the reaction value comes from the transition $^{25}\text{Mg}([5/2]^+_1) \rightarrow {}^{25}\text{Al}([5/2]^+_1)$, while the rest of $B(GT)$ values are very low and not reliable [20]. The nuclei ^{25}Mg and ^{25}Al are very deformed nuclei and the energy levels for these mirror nuclei are very well described by using the particle rotor model [20]. Theoretical calculations using USDA interaction have three five strong peaks located at $E_x(^{25}\text{Al})$= 0.0, 1.739, 6.213, 7.049 and 7.623 MeV, while the predicted USDB five strong peaks located at $E_x(^{25}\text{Al})$= 0.0, 1.72, 6.346, 7.132 and 7.922 MeV. The ground state of both ^{25}Mg and ^{25}Al nuclei are correctly predicted as $[5/2]^+$ by both USDA and USDB effective interactions. There are 40 calculated values of $B(GT)$ comes from the transitions $^{25}\text{Mg}([5/2]^+) \rightarrow {}^{25}\text{Al}(3/2^+, 5/2^+, 7/2^+)$ 12 of them are zero, 5 are strong peaks and the rest 23 are very small values

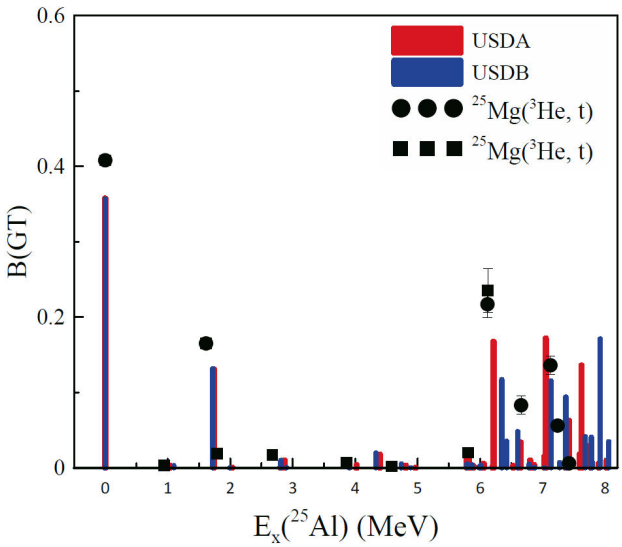

FIGURE 5. Shows the theoretical values of $B(GT)$ compared to the corresponding experimental data [22, 23] for ^{25}Mg.

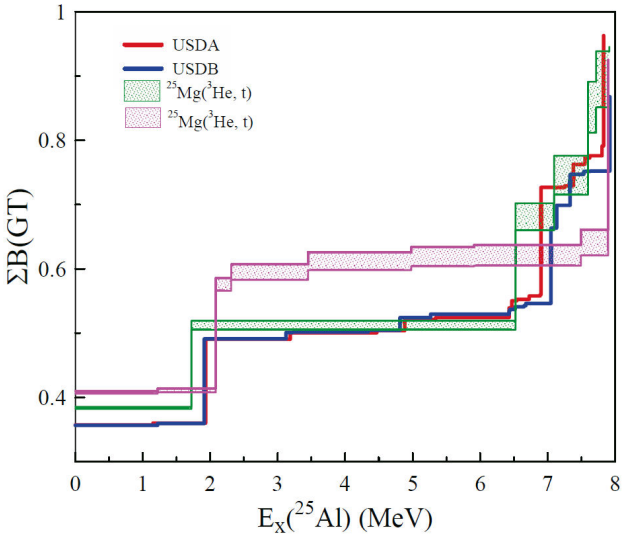

FIGURE 6. Shows the $\sum B(GT)$ distributions compared to experiment [22, 23] for ^{25}Mg.

predicted by both USDA and USDB interactions. The calculation of the accumulated $B(GT)$ strength values agreed very well with the data for ^{25}Mg (^{3}He,t) ^{25} Al [22] shown with green filled stripe, while the data taken from Ref. [23] with magenta color is not agreed with the theoretical predications of both USDA and USDB.

3.4. ^{26}Mg $\rightarrow$^{26}Al

Figure 6 shows the strength distribution of $B(GT)$ untruncated shell model calculations for the transition ^{26}Mg ($0^+ \rightarrow$ ^{26}Al (1^+) states using USDA and USDB interactions. The measured data obtained through the reaction of charge-exchange ^{26}Mg (^{3}He,t)^{26}Al [23, 24] up to the excitation energy E_x (^{26}Al) 7.24 MeV. The experimental data for the reaction ^{26}Mg (^{3}He,t)^{26}Al taken from Ref. [24]

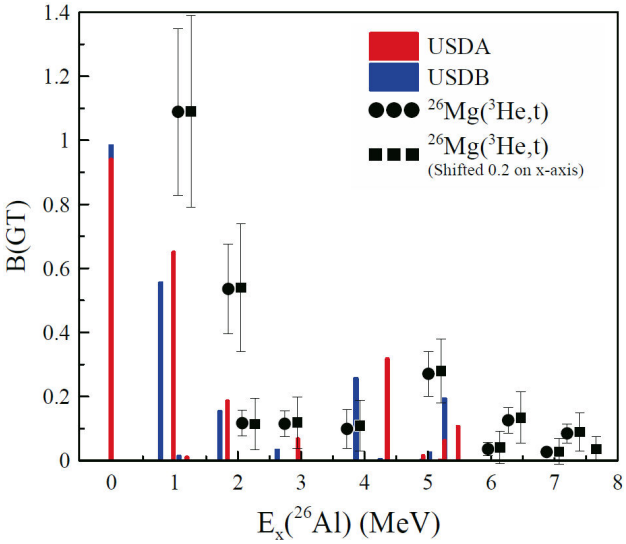

FIGURE 7. Shows the theoretical values of $B(GT)$ compared to the corresponding experimental data [23, 24] for for ^{26}Mg.

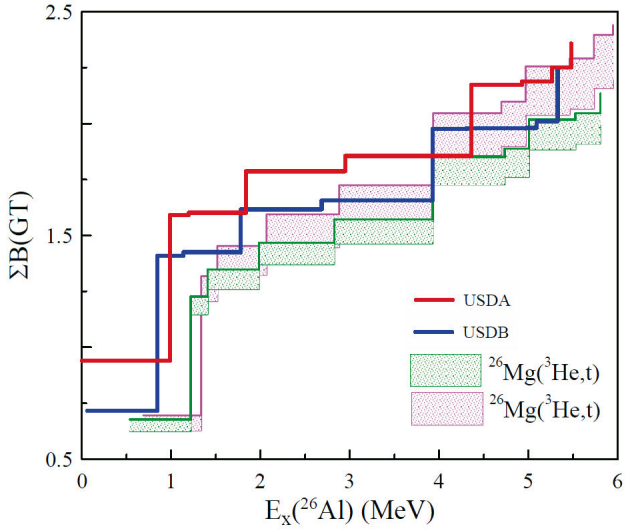

FIGURE 8. Shows the $\sum B(GT)$ distributions compared to experiment [23, 24] for ^{26}Mg.

shown with filled square pints are shifted by 0.2 MeV on the x-axis to not coincide with the data taken from Ref. [23] marked with filled circulus. There are two strong peaks for the experimental $B(GT)$ data from Ref. [23] located at 1.057 MeV and 1.85 MeV with values of 1.089 and 0.536, respectively, in the same manner, the data taken from Ref. [24] are very close in locations to the data of Ref. [23] which are located at 1.06 MeV and 1.85 MeV. Theoretical calculation with USDA predicts to strong peaks located at 0.0 MeV and 0.987 MeV, these strong peaks comes from the transition ^{26}Mg (0^+) $\rightarrow$^{26}Al(1_1^+) and ^{26}Mg (0^+) $\rightarrow$^{26}Al(1_2^+), respectively. In the same manner, the USDB two strong peaks located at 0.0 MeV and 0.783 MeV, which comes from transition ^{26}Mg (0^+) $\rightarrow$^{26}Al(1_1^+) and ^{26}Mg (0^+) $\rightarrow$^{26}Al(1_2^+), respectively. The accumulated $B(GT)$ strength values shown

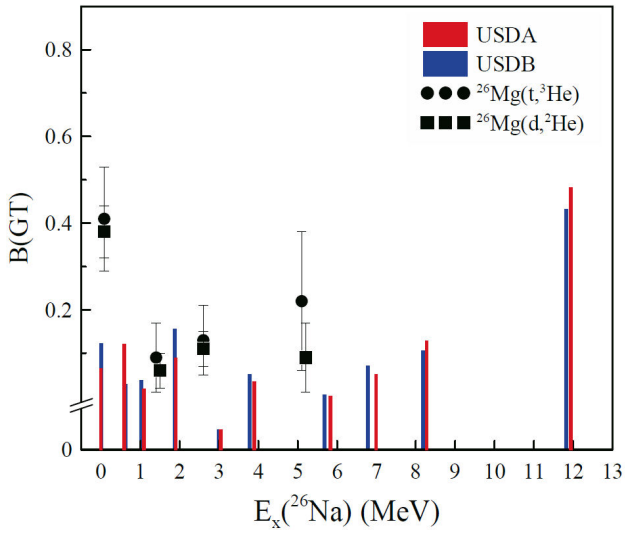

FIGURE 9. Shows the theoretical values of $B(GT)$ compared to the corresponding experimental data [23, 24] for ^{26}Mg.

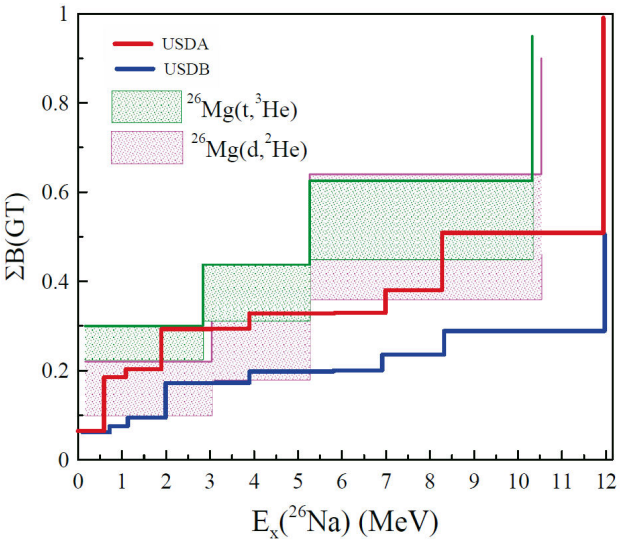

FIGURE 10. Shows the $\sum B(GT)$ distributions compared to experiment [23, 24] for ^{26}Mg.

in Fig. 7 determined by using both USDA and USDB effective interactions agrees very well with the measured data and the USDB interaction accumulated values of $B(GT)$ are more closer to the experiment than USDA.

3.5. ^{26}Mg $\rightarrow$^{26}Na

Figure 9 shows the GT transition strengths for the transition ^{26}Mg (0^+) ground state to (1^+) states. The experimental data observed from the reactions in ^{26}Na is available from a ^{26}Mg (t,^{3}He) experiment [23] and a ^{26}Mg(d,^{2}He) experiment [24] presented in Fig. 9, and the calculation of the shell-models in full sd model space using the USDA and USDB interactions, respectively. The strongest peak in the ^{26}Mg (t,^{3}He) reaction located at excitation energy $E_x(^{26}\text{Na})$= 0.08 MeV and for ^{26}Mg(d,^{2}He) reaction the strongest peak is located at also at $E_x(^{26}\text{Na})$= 0.08 MeV. There are only four experimental values for both ^{26}Mg(t, ^{3}He) and ^{26}Mg(d,^{2}He) reactions and they are distributed over excitation energy $E_x(^{26}\text{Na})$= 0.08-5.02 MeV. Theoretical calculations of USDA and USDB interactions reach to exciation energy $\sim$ 12 MeV. The USDA and USDB predicted the strongest peaks at 11.939 MeV and 11.82 MeV, respectively. The strongest experimental peaks comes from the transition ^{26}Mg $(0^+) \rightarrow ^{26}\text{Na}(1^+_1)$ for both ^{26}Mg (t,^{3}He) and ^{26}Mg (d,^{2}He) reactions which disagree with theoretical predictions which comes from the transition ^{26}Mg $(0^+) \rightarrow ^{26}\text{Na}(1^+_{10})$ for both USDA and USDB, while the rest of transitions gives weak $B(GT)$ strength distributions. The ground state spin and parity for both ^{26}Mg and ^{26}Na predicted correctly by both USDA and USDB interactions. Figure 10 displays the comparison of the accumulated sum of $B(GT)$ values predicted by USDA and USDB along with the corresponding measured data. The USDA interaction are better than USDB interaction to describe the running sum of $B(GT)$ values.

4. Conclusions

In this work we report the result of the shell model in the sd model space for the recent measured data of GT strengths of ^{24}Mg $\rightarrow$^{24}Na, ^{24}Mg$\rightarrow$^{24}Al, ^{25}Mg $\rightarrow$^{25}Al, ^{26}Mg$\rightarrow$^{26}Na, and ^{26}Mg$\rightarrow$^{26}Al transitions. The results of both USDA and USDB interactions show reasonable agreement wit the available measured data. Our conducted study add more information on the GT strength distributions obtained in earlier work. For the individual $B(GT)$ transitions, the qualitative agreement is obtained, while the predicted transition strengths sum is closely reproduced the observed data. This study might give useful information to researchers who are interested to study the $B(GT)$ transition strengths in this mass region.

1. F. Osterfeld, Nuclear spin and isospin excitations, *Rev. Mod. Phys.* **64** (1992) 491, https://doi.org/10.1103/RevModPhys.64.491.

2. A. L. Cole *et al.*, Gamow-Teller strengths and electron-capture rates for pf- shell nuclei of relevance for late stellar evolution, *Phys. Rev. C* **86** (2012) 015809, https://doi.org/10.1103/PhysRevC.86.015809.

3. P. Sarriguren, Contribution of excited states to stellar weak-interaction rates in odd- A nuclei, *Phys. Rev. C* **93** (2016) 054309, https://doi.org/10.1103/PhysRevC.93.054309.

4. A. Negret *et al.*, Gamow-Teller Strengths in the $A = 14$ Multiplet: A Challenge to the Shell Model, *Phys. Rev. Lett.* **97** (2006) 062502, https://doi.org/10.1103/PhysRevLett.97.062502.

5. K. Langanke and G. Martínez-Pinedo, Nuclear weak-interaction processes in stars, *Rev. Mod. Phys.* **75** (2003) 819, https://doi.org/10.1103/RevModPhys.75.819.

6. Y. Fujita, B. Rubio, and W. Gelletly, Spin-isospin excitations probed by strong, weak and electro-magnetic interactions, *Prog. Part. Nucl. Phys.* **66** (2011) 549, https://doi.org/10.1016/j.ppnp.2011.01.056.

7. K. G. Balasi, K. Langanke, and G. Martínez-Pinedo, Neutrino-nucleus reactions and their role for supernova dynamics and nucleosynthesis, *Prog. Part. Nucl. Phys.* **85** (2015) 33, https://doi.org/10.1016/j.ppnp.2015.08.001.

8. V. Kumar and P. C. Srivastava, Shell model description of Gamor-Teller strengths in pf-shell nuclei, *Eur. Phys. J. A* **52** (2016) 181, https://doi.org/10.1140/epja/i2016-16181-3.

9. V. Kumar, P. C. Srivastava, and H. Li, Nuclear β^--decay half-lives for fp and fpg shell nuclei, *J. Phys.*

G **43** (2016) 105104, https://doi.org/10.1088/0954-3899/43/10/105104.

10. T. Suzuki, M. Honma, H. Mao, T. Otsuka, and T. Kajino, Evaluation of electron capture reaction rates in Ni isotopes in stellar environments, *Phys. Rev. C* **83** (2011) 044619, https://doi.org/10.1103/PhysRevC.83.044619.
11. A. Saxena, P. C. Srivastava, and T. Suzuki, *Ab initio* calculations of Gamow-Teller strengths in the sd shell, *Phys. Rev. C* **97** (2018) 024310, https://doi.org/10.1103/PhysRevC.97.024310.
12. R. G. T. Zegers *et al.*, Spectroscopy of ^{24}Al and extraction of Gamow- Teller strengths with the ^{24}Mg(^{3}He, t) reaction at 420 MeV, *Phys. Rev. C* **78** (2008) 014314, https://doi.org/10.1103/PhysRevC.78.014314.
13. Y. Fujita *et al.*, $M1$ and Gamow-Teller transitions in $T = 1/2$ nuclei ^{23}Na and ^{23}Mg, *Phys. Rev. C* **66** (2002) 044313, https://doi.org/10.1103/PhysRevC.66.044313.
14. B. A. Brown and W. D. Rae, NuShell@MSU, MSU-NSCL Report, 2007 (unpublished).
15. B. A. Brown and W. A. Richter, New "USD" Hamiltonians for the sd shell, *Phys. Rev. C* **74** (2006) 034315, https://doi.org/10.1103/PhysRevC.74.034315.
16. L. Zamick and D. C. Zheng, Relations between Gamow-Teller and magnetic dipole transitions, *Phys. Rev. C* **37** (1998) 1675, https://doi.org/10.1103/PhysRevC.37.1675.
17. (duplicated reference, c.f. Ref. [12])
18. B. D. Anderson *et al.*, Gamow-Teller strength in the (p, n) reaction at 136 MeV on ^{20}Ne, ^{24}Mg, and ^{28}Si, *Phys. Rev. C* **43** (1991) 50, https://doi.org/10.1103/PhysRevC.43.50.
19. S. Rakers *et al.*, Gamow-Teller matrix elements from the ^{1}2C(d, ^{2}He) and ^{24}Mg(d, ^{2}He) reactions at 170 MeV, *Phys. Rev. C* **65** (2002) 044323, https://doi.org/10.1103/PhysRevC.65.044323.
20. Y. Shimbara *et al.*, Suppression of Gamow-Teller and $M1$ transitions in deformed mirror nuclei ^{25}Mg and ^{25}Al, *Eur. Phys. J. A* **19** (2004) 25, https://doi.org/10.1140/epja/i2003-10115-2.
21. Y. Fujita *et al.*, Evidence for the Existence of the $[2\ 0\ 2]\ 3/2$ Deformed Band in Mirror Nuclei ^{25}Mg and ^{25}Al, *Phys. Rev. Lett.* **92** (2004) 062502, https://doi.org/10.1103/PhysRevLett.92.062502.
22. R. G. T. Zegers *et al.*, The (t, ^{3}He) and (^{3}He, t) reactions as proves of Gamow-Teller strength, *Phys. Rev. C* **74** (2006) 024309, https://doi.org/10.1103/PhysRevC.74.024309.
23. K. Win, Y. Fujita, Y. Yeeoo, and H. Fujita, Analysis of high energy resolution data of ^{26}Mg(^{3}He, t)^{26}Al reaction, *EPJ Web Conf.* **206** (2019) 08003, https://doi.org/10.1051/epjconf/201920608003.
24. T. Niizeki *et al.*, Spin-isospin excitation in sd-shell nuclei studied by the (d, ^{2}He) reaction at $E_d = 270$ MeV, *Nucl. Phys. A* **577** (1994) 37, https://doi.org/10.1016/0375-9474(94)90831-1.